Elsevier Editorial System(tm) for Polymer Testing
Manuscript Draft

Manuscript Number:

Title: Effect of Nanoclay on Optical Properties of PLA/Clay Composite Films

Article Type: Original Paper

Keywords: ellipsometry, composites, nanoparticles and polylactide

Corresponding Author: Prof. Suprakas Sinha Ray,

Corresponding Author's Institution: DST/CSIR National Centre for Nanosctructured Materials

First Author: Suprakas Sinha Ray

Order of Authors: Suprakas Sinha Ray

Suggested Reviewers: Jasim Ahmed
jaahmed@kisr.edu.kw
One of the cited author

Bhesh Bhandari
b.bhandari@uq.edu.au
one of the expert in this field

Emmanuel Rotimi SADIKU
sadikur@tut.ac.za
one of the expert in this field

Opposed Reviewers:

Feb 3rd 2014

Editor
Polymer Testing

Dear Editor,

We wish to submit our recent article entitled as " Effect of Nanoclay on Optical Properties of PLA/Clay Composite Films" for possible publication in *Polymer Testing* as a regular article.

The objective of this study was to investigate the effect of organically modified montmorillonite (OMMT) clay loadings on the optical properties of PLA. To date, studies investigating the use of PLA for microcantilever applications have not been reported. The surface morphology of the PLA/clay composite was studied using scanning electron microscopy (SEM) and atomic force microscopy (AFM). Transmission electron microscopy (TEM) was used to study the dispersion of the silicate layers in the PLA matrix. The dispersion of nanoparticles is important for optical studies to understand the interaction between light and the surface of the polymer composite. The optical properties of the PLA were studied using spectroscopic ellipsometry and supplemented with ultra-violet visible spectroscopy.

It would be the greatest pleasure for us if the work could be accepted for publication in such an eminent journal as yours.

The manuscript is original and not submitted previously for publication in any form.

Thanking you in advance for favorable consideration.

I am looking forward to hearing from you at your earliest convenience.

With best regards,

Sincerely yours,

Professor Suprakas Sinha Ray
On behalf of all authors

Effect of Nanoclay on Optical Properties of PLA/Clay Composite Films

H.M. Cele,[a, b] V. Ojijo,[a] H. Chen,[a] S. Kumar,[a] K. Land,[a] T. Joubert,[a] M.F.R. de Villiers,[a] S. S. Ray* [a, b, c]

[a] *Material Science and Micro-Manufacturing, Council for Scientific and Industrial Research, 1-Meiring Naude Road, Brummeria, Pretoria 0001, South Africa*
[b] *Department of Applied Chemistry, University of Johannesburg, Doornfontein 2018, Johannesburg, South Africa*
[c] *DST/CSIR National Centre for Nanostructured Materials, Council for Scientific and Industrial Research, 1-Meiring Naude Road, Brummeria, Pretoria 0001, South Africa*

ABSTRACT

This article reports the modification of optical properties of biodegradable/biocompatible polylactide (PLA) using organically modified montmorillonite (OMMT) for microcantilever applications. PLA/OMMT composite films with various OMMT loadings (3, 5 and 7 wt%) were prepared using solvent casting. The surface morphologies of the PLA/OMMT composites were examined using scanning electron and atomic force microscopes. The morphological results indicated that the surface roughness increases as a function the clay load. The optical properties of the PLA/OMMT composites were studied using variable angle spectroscopic ellipsometry (VASE) and ultra-violet (UV-Vis) spectroscopy. VASE revealed that the refractive index and extinction coefficient (*n* and *k*) positively correlated with the thickness of the film. UV-Vis spectroscopy also demonstrated that the absorption of light by PLA/OMMT composite films positively correlated with the clay content in the visible range of the electromagnetic spectrum. To enhance the reflectivity, PLA/OMMT films were coated with a gold layer.

Keywords: ellipsometry, composites, nanoparticles and polylactide

1. **Introduction**

Polylactide (PLA) is an environmentally benign [1, 2] thermoplastic derived from lactic acid [2, 3]. The structure of PLA is unique compared to other polymers, and it can consist of enantiomers of both L- and D-lactide as repeating units [2]. PLA was employed for this study due to its favourable properties, such as biocompatibility and high mechanical strength [4-6]. The incorporation of fillers can reportedly improve the mechanical properties of PLA [4, 7, 8]. Nano-reinforcements are mainly used in nanocomposites due to their enhanced properties, including their mechanical strength and thermal stability [4-6].

Despite the favourable properties, the inherent brittleness of PLA rigorously limits its more widespread implementation [9]. The prospective applications of PLA in the field of biomedical materials are broad due to its biocompatibility [9]. PLA holds tremendous promise as an alternative material for the production of transducers, such as microcantilevers. Microcantilevers could be used as biosensors to bind specific biomolecules. Various detection methods are used to detect the binding of biomolecules by measuring the deflection of the microcantilever. Optical readout is one of the detection methods that is commonly used to measure and monitor the deflection of microcantilevers with extremely high accuracy. This method can operate either in static or dynamic mode by shining a laser beam on the surface of the cantilever [10-14]. The deflection of the cantilever beam is measured, often by monitoring the position of the laser beam. Therefore, a microcantilever requires a reflective surface for deflection measurements.

The optical behavior of PLA thin films has not been extensively studied. Few studies have been reported on the optical studies of PLA and modified PLA. Hutchinson *et al.* [2] optically studied PLA using spectroscopic ellipsometry. This study was performed to understand the behavior of a neat PLA at a wavelength of 300-1300 nm for packaging applications. The authors performed ellipsometric measurements on a well-characterised set of homopolymers and copolymers to cover a wide range of stereoisomer proportions and L-contents. They expected the index of refraction to be constant for each PLA structure and thickness. However, spectroscopic ellipsometry measurements revealed that the refractive index significantly depended on the PLA film thickness. Hiroi *et al.* [15] produced PLA nanocomposites (PLANCs) by adding the organically modified layered titanate as a nanofiller. Optical studies showed that the visible region changed compared to the neat PLA as the absorbency increased due to the presence of titanate layers.

However, the material properties of PLANCs, including the degradability, significantly improved when exposed to sunshine.

In this work, considerable efforts have been made to modify the optical properties of PLA using nanofillers to suit the microcantilever applications. The incorporation of nanoclay could positively alter the optical properties of PLA in various applications, such as microcantilevers, where the reflection is needed. Therefore, studying the effect of clay nanoparticles on the optical properties of PLA is necessary.

The objective of this study was to investigate the effect of organically modified montmorillonite (OMMT) clay loadings on the optical properties of PLA. To date, studies investigating the use of PLA for microcantilever applications have not been reported. The surface morphology of the PLA/clay composite was studied using scanning electron microscopy (SEM) and atomic force microscopy (AFM). Transmission electron microscopy (TEM) was used to study the dispersion of the silicate layers in the PLA matrix. The dispersion of nanoparticles is important for optical studies to understand the interaction between light and the surface of the polymer composite. The optical properties of the PLA were studied using spectroscopic ellipsometry and supplemented with ultra-violet visible spectroscopy.

2. Experimental

2.1. Materials

The PLA used in this study was of commercial grade (PLA 2002D) with a D-isomer content of approximately 4 % and was obtained from Natureworks, LLC (USA). The average molecular weight, density, glass transition temperature and melting temperature of the PLA were 235 $Kg.mol^{-1}$, 1.24 $g.cm^{-3}$, approximately 60 °C and 153 °C, respectively. The filler used for this experiment was an OMMT (commercially known as Cloisite® 30B, C30B), which was purchased from Southern Clay Products, USA. According to the supplier, the pristine MMT was modified with 30 wt% of methyl tallow bis (2-hydroxyethyl) quaternary ammonium salt. The chloroform used in this study was purchased from Sigma Aldrich, South Africa.

2.2. Sample Preparation

2.2.1. Neat PLA thin film

The polymeric solutions were prepared from PLA pellets using chloroform. A known weight of PLA (10 g) was dissolved in 200 ml of chloroform at room temperature for 5 h. The viscosity of the polymeric solution was controlled by varying the volume of the solvent. The polymeric thin films were prepared by casting a polymer solution on a glass slide using a spin coater, model G3P-8 (specialty coating systems, USA). The calibration of the spin curves was investigated at different rotation speeds (100-6000 rpm). The solvent was evaporated at room temperature for 12 h.

2.2.2. PLA/C30B composite film

For consistency, a similar experiment using the method described above was performed with the incorporation of C30B particles. Different concentrations (3, 5 and 7 wt.%) of C30B of the total weight (W_{PLA} and W_{C30B}) were incorporated into a PLA solution, which were then ultrasonically mixed for 3 h at 40 °C. A non-homogeneous solution was obtained from this experiment, and a magnetic stirrer was used to improve the homogeneity of the solution. The homogenous PLA-C30B solutions were then spin coated at 1000 rpm for 2 min and dried at room temperature. Samples were labelled as PLA-3C30B, PLA-5C30B and PLA-7C30B for 3, 5 and 7 wt.% of C30B loading, respectively.

2.2.3. Gold coating

A gold (Au) layer (55 ± 2 nm) was deposited on the PLA-C30B films using the AJA International, Inc sputtering system (AJA International, USA). Au coating was performed to prevent PLA from transmitting or absorbing light and to increase the reflectivity.

2.3. Characterisation methods

The surface morphology of neat PLA (reference film), PLA-C30B and Au-coated PLA-C30B films was studied using SEM (FIB-SEM Auriga Zeiss). Surface roughness of PLA/C30B films was measured using a Multimode AFM Nano Scope Version IV (Bruker, USA). A tip with a radius curvature of less than 10 nm was used for imaging. The tip was mounted on a 125 µm long cantilever with a spring constant of 40 N/m and was employed in the tapping mode experiment. Both the height and phase images were obtained using a scan rate of 0.5 Hz and tip frequencies ranging from 280 – 310 kHz.

Variable angle spectroscopic ellipsometry (VASE) measurements were performed using a J.A. Woollam M200SE (USA) with an auto-retarder (rotating analyser ellipsometer with a computer-controlled Berck wave plate, which removes the errors in Δ encountered near 0 and 180°). The data were obtained between 300 and 1000 nm in 5 nm steps and incident angles (AOI) of 65, 70 and 75°. For data analysis, the films were regarded as a homogeneous material with a film thickness modelled using a Cauchy model [16]. A B-Spline model [17, 18] was then used to extract the refractive index (*n*) and extinction coefficient (*k*) over the absorption range from 300 to 1000 nm.

An ultra violet visible spectrophotometer (Perkin-Elmer Lambda 750S, USA) was used to characterise the absorption properties of the PLA and PLA composite films in the 200–900 nm wavelength range at room temperature.

3. Results and Discussion

3.1. Surface morphology studies

Figure 1 shows SEM images of the neat PLA and PLA-C30B composite films. The SEM image of the neat PLA film in Figure 1a shows a uniformly deposited film with a smooth surface. Part (a) to (d) of Figure 1 show the SEM images of composite films that were prepared from the ultrasonically mixed PLA-C30B solution. The SEM images of these PLA-C30B composites showed that some clay nanoparticles lay on the surface of the film. The particles seemed to be agglomerated on the surface of the composite film. The clustering of clay particles was randomly distributed [19], suggesting that the sizes of clusters were irregular. Agglomerated nanoparticles were also observed, but the number of C30B nanoparticles on the surface was expected to increase as the C30B concentration increased. Despite the variation in the C30B concentration, the SEM images showed a similar surface morphology for all the PLA/C30B composite films. This similarity indicates that the particles cluster at different areas of the film, which may be due to the mixing process. In this case, the incorporation of C30B particles affects the mechanical properties of the entire film [20]. Well dispersed clay particles are extremely important for the consistency of mechanical properties for microcantilever applications. However, undesirable bubbles were also obtained due to the mixing process. These bubbles should be avoided by not spin coating the PLA solution immediately after mixing to obtain a uniform film, which is also favourable for

microcantilever applications. The surface morphology of PLA-C30B films covered in an Au layer was also inspected using AFM. The resultant images showed a smooth surface.

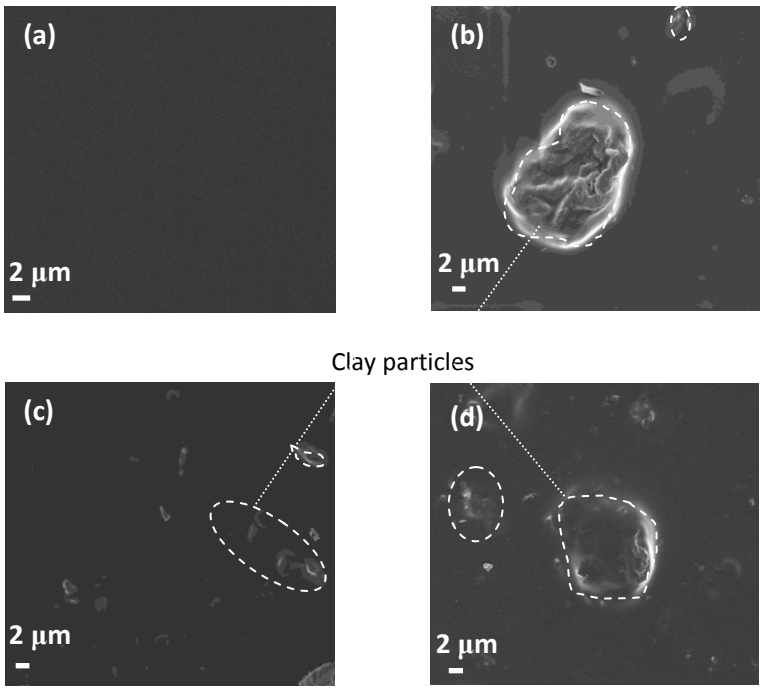

Figure 1. SEM images of PLA composite prepared by spin coating (a) neat PLA), (b) PLA-3C30B, (c) PLA-5C30B and (d) PLA-7C30B.

To supplement the SEM analysis, the average surface roughness of PLA and PLA-C30B composite films was measured directly from the surface of the film using AFM. The average roughness of a neat PLA was found to be 0.963 nm. However, the surface roughness of the PLA-3C30B, PLA-5C30B and PLA-7C30B composite films increased as depicted in **Table 1** upon the addition of C30B particles. AFM analysis revealed that the surface roughness is directly proportional to the concentration of clay particles. These findings are consistent with those of Xu *et al.* [21]. The AFM images in **Figures 2**(b-d) show brighter regions with dotted circles that represent the clay particles closer to the AFM tip. However, the surface roughness was not uniform throughout the entire film, which confirms that the particle sizes differed. Therefore, surface imaging was performed at different areas of the film. An increase in the surface roughness of the PLA-C30B composite is associated with agglomerated clay particles.

Table 1. The AFM measured root mean square and average roughness of neat PLA, PLA-3C30B, PLA-5C30B, PLA-7C30B.

Sample	**Root mean square** Rq (nm)	**Average roughness** Ra (nm)
Neat PLA	1.66	0.96
PLA-3C30B	20.13	10.15
PLA-5C30B	21.15	14.56
PLA-7C30B	96.40	63.01

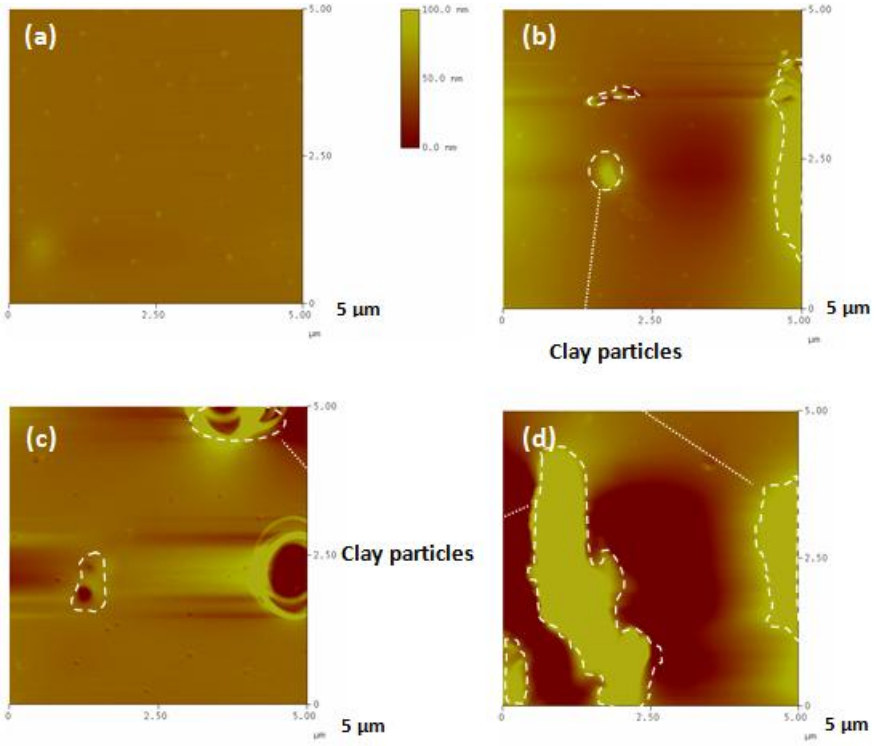

Figure 2. AFM images of PLA with the different loadings of clay particles. (a) neat PLA, (b) PLA-3C30B, (c) PLA-5C30B and (d) PLA-7C30B

3.2. Clay distribution analysis

To further investigate the distribution of clay platelets in the PLA matrix, a high resolution TEM analysis was carried out. The TEM images of the PLA-C30B composites revealed a random distribution of clay particles. **Figure 3** shows the random distribution of clay particles across the film. The non-uniform distribution of particles is undesirable to maintain consistent mechanical properties of the film. If agglomeration is unavoidable, it should be uniform (same size of clusters throughout the film) or clay particles should be exfoliated into the PLA matrix. Wang *et al*. [21]

reported agglomerated organoclay in the PLA matrix, which was associated with clay layers being torn apart from clay bundles. The exfoliated clay particles were desired due to the consistency of the mechanical properties of composite film [20]. Despite the agglomeration, PLA is intercalated between silicate galleries. This intercalation seemed to be anisotropic in the composites, as shown in parts (a) to (c) of Figure 3.

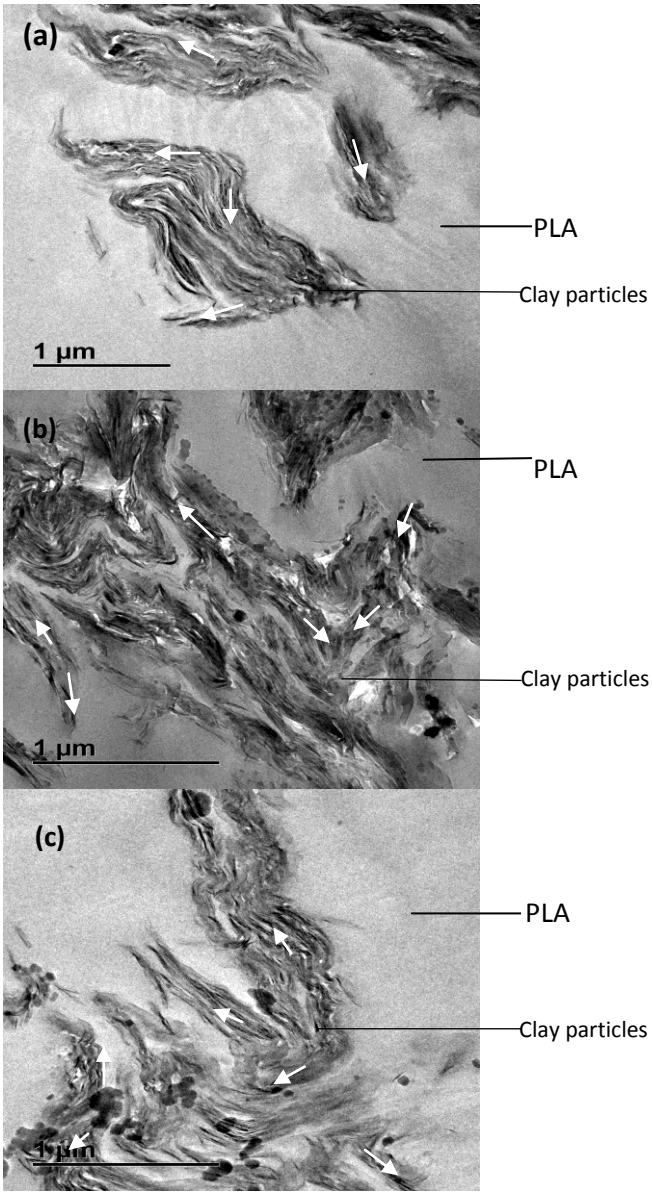

Figure 3. TEM images showing the intercalated PLA into the clay galleries: (a) PLA-3C30B, (b) PLA-5C30B and (c) PLA-7C30B.

3.3. Optical analysis

The optical properties of PLA have typically been elucidated using VASE and UV-Vis. VASE offers a qualitative understanding of the *n* and *k* of PLA as the clay particles are added to the PLA matrix. Conversely, UV-Vis provides direct evidence of the PLA film transmitting, absorbing or reflecting light after the addition of clay.

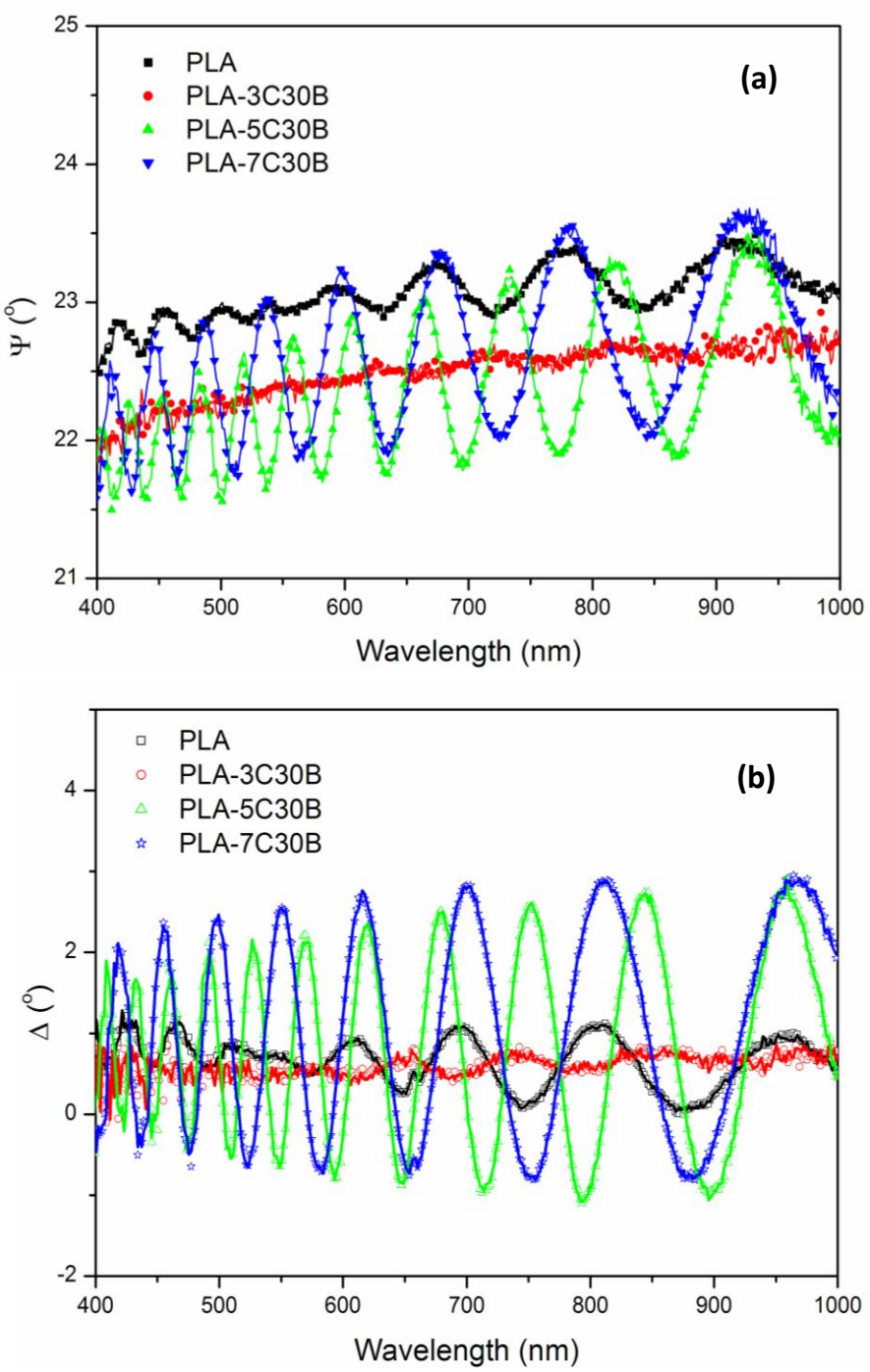

Figure 4. Measured ellipsometry parameters (solid lines) and modeled calculation results (dashed lines) of (a) ψ and (b) Δ as a function of wavelength for PLA and PLA with different clay loadings at 70°.

To obtain the optical constants (*n* and *k*) of the PLA-C30B composite films, the ellipsometry parameters ψ and Δ were experimentally measured as a function of the wavelength at a 70° AOI. **Figure 4** shows that the fits of model calculation (solid lines) closely approximated the experimental data (dotted lines). Figure 4a demonstrates that the value of ψ increased upon the addition of clay to the PLA matrix. We attribute this increase to the improved crystallisation of PLA as observed in the UV-vis results (Figure 8), which showed a red shift and a more intense peak; these changes confirm the phase transition to a crystalline ordering state. The changes observed from the ellipsometric spectra upon the incorporation of clay reflected the changes in the electronic structure of the material. These changes might be induced by the electrical forces (the strong electrical field at the vicinity of PLA/C30B interfaces), which in turn modify the optical properties of the composite.

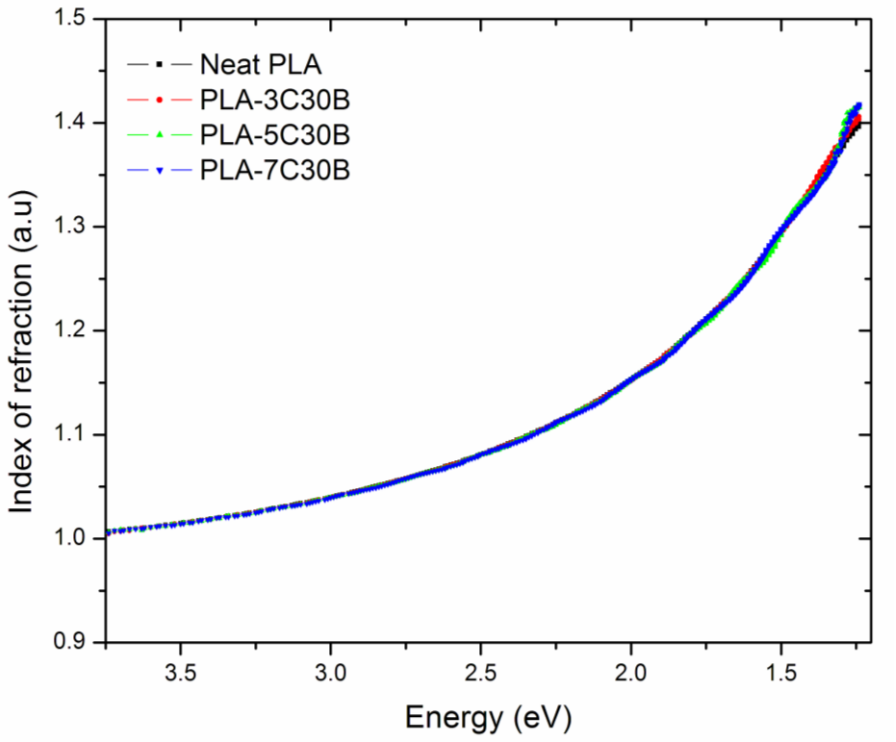

Figure 5. Index of refraction of PLA with different clay loadings.

To further investigate the effect of clay nanoparticles on the optical properties, the refractive index was measured with respect to various clay loads. **Figure 5** depicts the extracted *n* values of

the PLA and PLA-C30B composite films as a function of energy. Figure 5 shows that the *n* values of the PLA film increased from 1.1 to 1.41 between 3.75 and 1.2 eV. This increase in the *n* values of the PLA-C30B composite films could be due to the partial crystallisation induced by clay, which results in a reorganisation of the polymer chains due to the shift in the UV-vis spectrum (Figure 8). Figure 5 indicates that the clay nanoparticles enhance the crystallisation of PLA and the absorption of light by PLA-C30B. The C30B load did not affect the refractive index. This behaviour of composites could be due to the slight variation in the thickness (**Table 2**), i.e., thicker films could result in a significant variation of the refractive index. For microcantilever applications, the clay concentration should be minimised to obtain stable and flexible cantilever beams.

Table 2. Films parameters extracted from both PVD and SE analysis

Films	**Thickness determined from the thickness monitor** (nm)		**Thickness from SE** (nm)	**MSE**	**Thickness from FIB SEM**
Au	55.32		55.54	8.13	-
PLA	-		2315.4	0.437	1400
PLA-***3***C30B	-		2319.0	5.803 e-9	1600
PLA-***5***C30B	-		2324.6	0.122	1700
PLA-***7***C30B	-		2325.0	1.434	-
PLA-***5***C30B-Au	PLA	-	2324.6	0.430	-
	Au	55.3	55.50	8.001	-

Figure 6 indicates that the extinction coefficient of the PLA film at 3.75-1.2 eV increases as the clay load increases. The intensity of the absorption peak also increases as the energy decreases (3.75 to 1.2 eV), and the strongest optical absorptions occurs at 1.3 eV [22]. A red shift near 1.625 eV and an increase in the absorption peaks were observed when the clay particles infiltrated the PLA matrix. These changes might be the result of the self-organisation and crystallisation of PLA molecules into an extended molecular conformation that increases the electronic conjugation length. Moreover, the number of interference fringes also increased as clay nanoparticles were added to the PLA matrix. The increase in the amplitude of interference fringes is associated with an improvement in the *k* values.

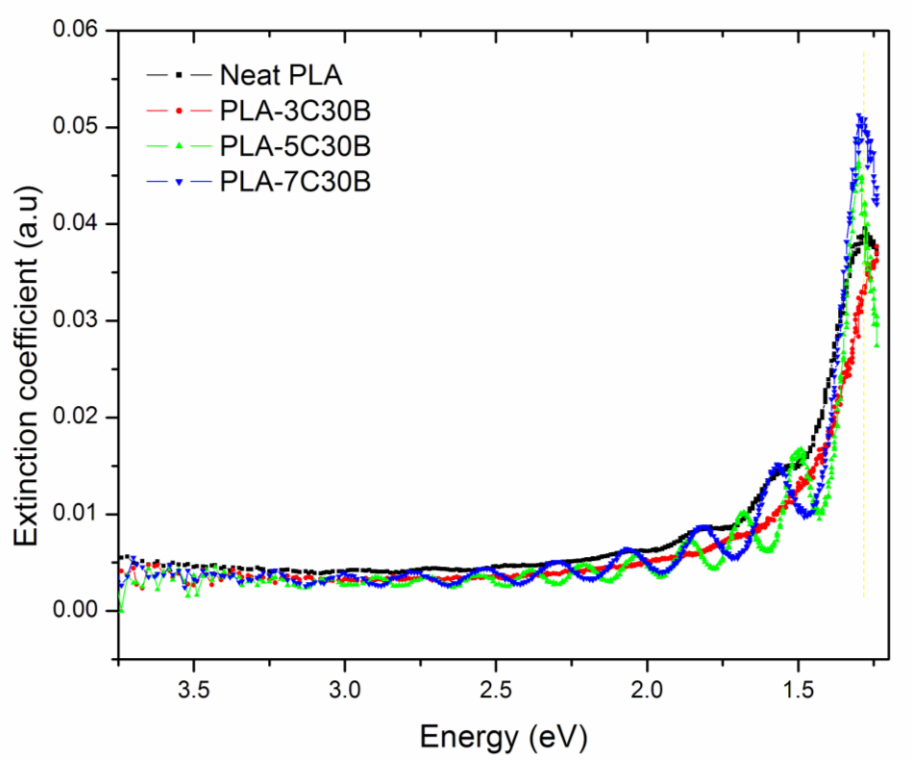

Figure 6. Extinction coefficient of PLA/Clay composite films as a function of wavelength.

Figure 7 shows the UV-Vis spectra of the neat PLA and the PLA infiltrated with different clay loads. The transmittance of the neat PLA in Figure 7 was approximately 85 % and decreased as clay particles were added to the PLA matrix. The reduction in transmittance is possibly related to the thickness of the PLA, as revealed by VASE. The decrease in the transmittance could also be due to the presence of clay nanoparticles, because light interacts with clay particles and some of the particles could absorb some of the energy. This phenomenon can be attributed to the agglomeration trend with respect to the clay loads [21] as well as the dispersion of the nanoparticles. Moreover, a red-shift was observed at 300-350 nm, which was directly proportional to the clay loads. This red shift is consistent with the ellipsometric results observed in Figure 6. This finding is consistent with the findings by Fukushima *et al.*[23], who showed that the transmission of PLA with OMMT nanocomposites reduced as a function of the wavelength from 380 to 780 nm. Based on their observations, the transmittance of PLA/clay composites depends on the dispersion and type of nanoparticles. The absorbance of the film increased in the visible range upon the addition of OMMT to the PLA matrix [23].

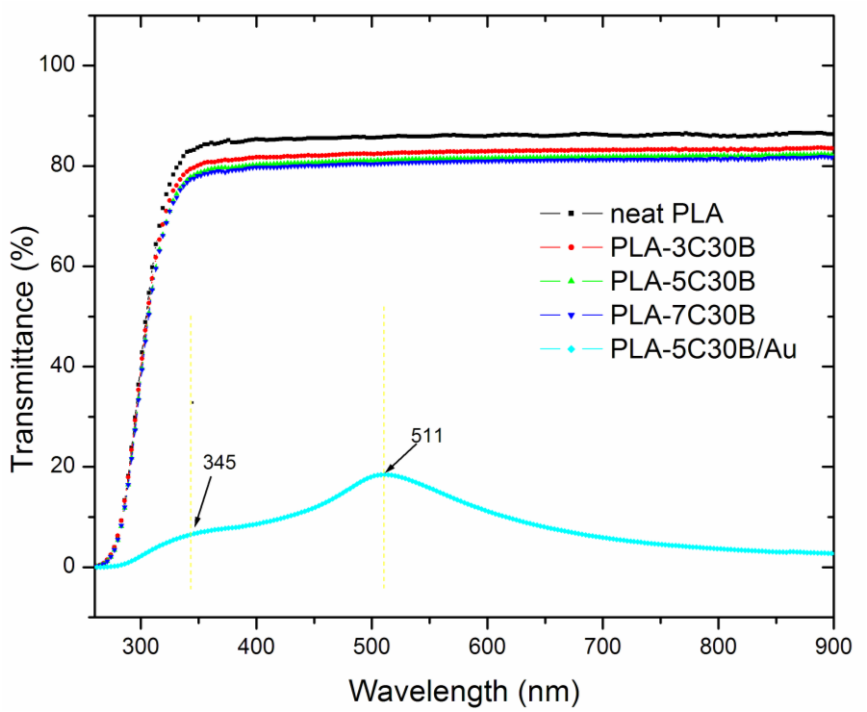

Figure 7. UV-Vis measurements (transmittance) of PLA, PLA-3C30B, PLA-5C30B, PLA-7C30B and Au/PLA-5C30B.

Au-coated PLA shows a peak at 511 nm and a shoulder near 345 nm. The intense peak indicates the presence of an Au layer that is normally found at a wavelength of 520 nm due to the surface plasmon [24]. Similar results were found by Siegel *et al*.[25], who showed an absorption peak of Au film (<20 nm thick) at 500 nm. The peak could slightly shift to the high or low wavelengths, depending on the film thickness. Therefore, the absorption band is broadened as the thickness of the Au layer increases due to a wider particle size distribution [25].

Figure 8 shows the extrapolations of the optical band gap of PLA as a function of the clay load in the PLA matrix. The direct band gap obtained for the neat PLA in **Table 3** is 4.513 eV. The band gap was expected to decrease linearly as the weight percentage of C30B increased because more electrons can jump to the conduction band within a small energy change as more C30B is added. The decrease in the band gap of composites shows that the conductivity of PLA decreases as the clay nanoparticles are incorporated. Nevertheless, the conductivity of the polymer is not that crucial for microcantilever applications when using optical readout. The conductivity of the polymer could be essential in other forms of the readout, such as the piezoresistive or capacitive

deflection readout [11]. Moreover, the effect of clay nanoparticles on the conductivity of PLA seemed to be very minimal at low concentrations. These values indicate that the clay load had influenced the experimental band gap value of PLA-C30B composite films.

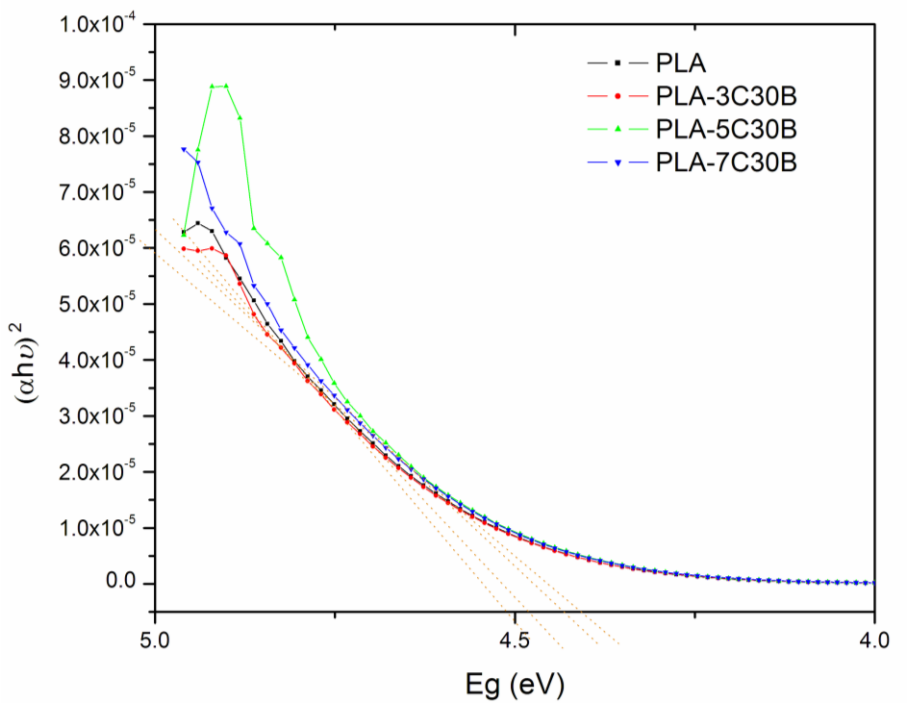

Figure 8. Direct gap graphs ($(\alpha hv)^2$ vs. hv) of PLA/Clay composite.

Table 3: Direct band gap of PLA/Clay composite thin films.

Clay loading (wt%**)**	**Band-gap (**eV**)**
0	4.51
3	4.48
5	4.44
7	4.40

The indirect band-gap values are shown in **Table 4** and demonstrate a behaviour similar to that of the direct band-gap for 0 to 7 wt.% loads. The indirect band gap plot (**Figure 9**) indicates a slight variation of the band gap, which can be associated with the dispersion of nanoparticles. The mixing process could have had an influence on the dispersion rate of clay nanoparticles inside the PLA matrix, which affects the band gap of the PLA-C30B composite film. The band gap of PLA

evidently decreases as the concentration of C30B increases when clay nanoparticles are incorporated into the PLA matrix.

Table 4 : Indirect band gap for PLA/Clay composite thin films

Clay loading (wt%)	**Band-gap** (eV)
0	3.74
3	3.72
5	3.71
7	3.70

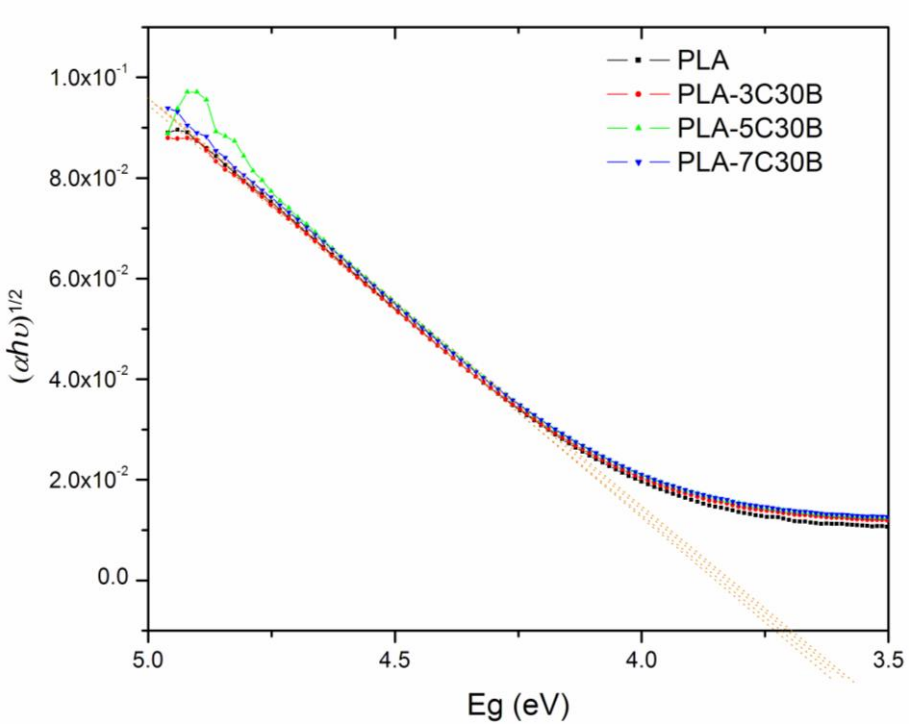

Figure 9. Indirect band gap graphs ($(\alpha hv)^{1/2}$ vs. hv) of PLA/Clay composite.

The reflectance of PLA upon the addition of clay nanoparticles was measured to supplement the transmittance results. Figure 10a depicts the reflectance spectra of PLA, PLA-C30B and Au-PLA-C30B films. Interference fringes were observed in PLA and PLA-C30B films, as shown in the magnified spectra in Figure 10b. These interference fringes could be due to the interaction of the reflected light from the PLA surface with the reflected light from the substrate. The UV-Vis spectra showed the most intense PLA peak at a wavelength of 311 nm, which indicates that a

neat PLA is reflecting light in this range. Red-shift near 345 nm is observed at low concentrations of C30B (3 and 5 wt.%), and the peak reflection decreases as the clay concentration increases. Blue-shift is observed as the clay concentration was increased to 7 wt.%. The sharpness of the sub-peak of PLA from the visible range also decreased after the incorporation of clay. Therefore, clay particles increase the absorption of light by PLA in the visible range. After coating the PLA/C30B composite with a 55 Au layer, an intense peak was found at 678 nm, which is associated with the reflection of light by the Au layer. The Au layer improved the reflectivity of the composite at the visible range.

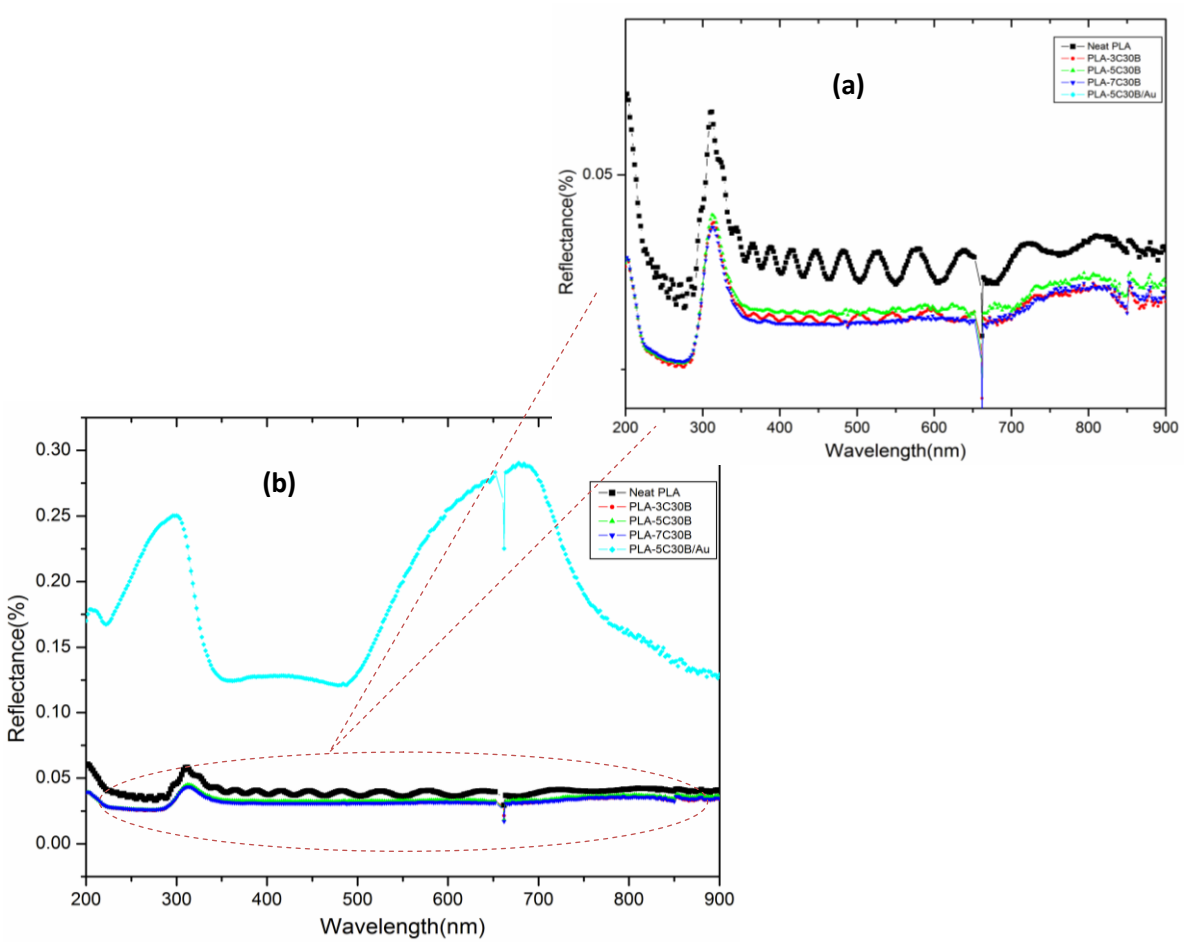

Figure 10. UV-vis reflectance as a function of wavelength. (a) Reflectance of PLA with different clay loadings and Au coated PLA/Clay composite (b) the magnified reflectance of PLA and PLA/Clay composites.

4. Conclusions

PLA-clay composite films were prepared by the incorporation of modified clay particles into PLA solutions. SEM images show that the surface of neat PLA is smooth compared to the PLA-clay composite. The AFM analysis revealed that the surface roughness of the PLA-clay film increases as the clay concentration increases. A non-uniform surface roughness was obtained, which was associated with the aggregation of clay particles. Furthermore, high resolution TEM revealed anisotropic intercalated PLA chains between the clay galleries.

The refractive index, *n*, and the extinction coefficient, *k*, were determined using the Cauchy model. Spectroscopic ellipsometry revealed that optical constants depend on the thickness of the film. The UV-Vis measurements showed that a neat PLA transmits light in the visible light region. As nanoparticles were added to the matrix, a red-shift and reduction in transmittance were obtained. The reduction in the transmittance is due to the absorption of light by clay particles. However, the UV-Vis measurements revealed that the transmittance and reflectance significantly depended on the thickness of the composite films. After Au-coating, both the VASE and UV-Vis measurements demonstrated the improvement in the reflective property of the polymer composite. Therefore, these films can be used to fabricate biosensors (e.g. microcantilevers). For cantilever beams, exfoliated clay particles are suggested to improve the thermal and mechanical properties. Finally, developing a method that will produce exfoliated nanoparticles to improve the surface morphology and surface reflectance remains a challenge.

Acknowledgments

The financial support by Department of Science and Technology (DST, South Africa), Council for Scientific and Industrial Research (CSIR, South Africa) and Technology Innovation Agency (TIA, South Africa) is gratefully acknowledged. We also thank D.E. Motaung, G.F. Malgas and T. Malwela for the helpful discussions.

References

[1] S. S. Ray, K. Yamada, M. Okamotoa, K. Ueda, Polymer 44 (2003) 857–866.

[2] M.H. Hutchinson, J.R. Dorgan, D.M. Knauss, S.B. Hait, J. Polym. Environ. 14 (2006) 119–124.

[3] A. Jasim, V. K. Sunil, Intern. J. Food Propert. 14 (2011) 37-58.

[4] V. Ojijo, H. Cele, S. S. Ray, Macromol. Mater. Eng. 296 (2011) 865-877.

[5] S. S. Ray, M. Bousmina, Prog. Mater. Sc. 50 (2005) 962-1079.

[6] S. S. Ray, M. Okamoto, Prog. Polym. Sci. 28 (2003) 1539-1641.

[7] S. S. Ray, K. Yamada, M. Okamoto, A. Ogami, K. Ueda, Chem. Mater. 15 (2003) 1456-1465.

[8] S. S. Ray, M. Bousmina, Macromol. Rapid. Communs. 26 (2005) 1639-1646.

[9] L. Feng, X. Bian, Z. Chen, G. Li, X. Chen, Polym. Degrad. Stabil. 98 (2013) 1591-1600.

[10] L.G.V. Torrijo, Development of Cantilevers for Biomolecular Measurements, in, Universitat Autonoma de Barcelona, 2006, pp. 1-261.

[11] A. Boisen, S. Dohn, S.S. Keller, S. Schmid, M. Tenje, Reports Prog. Phys. 74 (2011) 036101.

[12] M. Nordström, S. Keller, M. Lillemose, A. Johansson, S. Dohn, D. Haefliger, G. Blagoi, M. Havsteen-Jakobsen, A. Boisen, Sensors, 8 (2008) 1595-1612.

[13] A.W. McFarland, Production and Analysis of Polymer Microcantilever Parts, in: George W. Woodru® School of Mechanical Engineering, Georgia Institute of Technology, 2004, pp. 1-307.

[14] P. Urwyler, H. Schift, J. Gobrecht, O. Häfeli, M. Altana, F. Battiston, B. Müller, Sensors and Actuators A: Physical, 172 (2011) 2-8.

[15] R. Hiroi, S.S. Ray, M. Okamoto, T. Shiroi, Macromol. Rapid Communs. 25 (2004) 1359-1364.

[16] U. Zhokhavets, G. Gobsch, H. Hoppe, N.S. Sariciftci, Synth. Met. 143 (2004) 113-117.

[17] J.W. Weber, T.A.R. Hansen, M.C.M.v.d. Sanden, R. Engeln, J. Appl. Phys. 106 (2009) 123503-123503.

[18] B. Johs, J.S. Hale, Phys. Status Solidi A, 205 (2008) 715-719.

[19] S. S. Ray, K. Yamada, M. Okamoto, Y. Fujimoto, A. Ogami, K. Ueda, Polymer 44 (2003) 6633-6646.

[20] Q.T. Nguyen, D.G. Baird, Adv. Polym. Technol. 25 (2006) 270–285.

[21] S. Wang, Y. Zhang, W. Ren, Y. Zhang, H. Lin, Polym. Test. 24 (2005) 766-774.

[22] Y.W. Jung, J.S. Byun, Y.H. Cha, Y.D. Kim, Synth. Met. 160 (2010) 651-654.

[23] K. Fukushima, A. Fina, F. Geobaldo, A. Venturello, G. Camino, eXPRESS Polym. Letts. 6 (2012) 914–926.

[24] S. SRIVASTAVA, M. HARIDAS, J.K. BASU, Indian Academy Sci. 31 (2008) 213–217.

[25] J. Siegel, O. Lyutakov, V. Rybka, Z. Kolská, V. Švorčík, Nanoscale Res. Letts. 6 (2011) 1-9.